Inorganic Chemistry

Article

pubs.acs.org/IC

$LaCo_{1-x}Ni_xO_3$ with Improved Electrical Conductivity

Hisashi Kozuka,*[,†,‡] Kazushige Ohbayashi,[†] and Kunihito Koumoto[‡]

[†]NGK Spark Plug Co., Ltd., 2808, Iwasaki, Komaki-shi, Aichi 485-8510, Japan

[‡]Department of Applied Chemistry, Graduate School of Engineering, Nagoya University, Furo-cho Chikusa-ku, Nagoya 464-8603, Japan

ABSTRACT: To determine the applicability of $LaCo_{1-x}Ni_xO_3$ in a conductive material for electrical wiring, the dependence of the electronic transport property on the Ni content is investigated via Hall effect measurements, Rietveld analyses, and band-structure calculations. Ni doping (50 mol %) into the Co sites realizes a high electrical conductivity of 1.9×10^3 S/cm, which is an unexpectedly high value for a $LaCo_{1-x}Ni_xO_3$ system, at room temperature due to the high carrier concentration of 2.2×10^{22} cm^{-3} and the small effective mass of 0.1 m_e. In addition, the high electrical conductivity is maintained from room temperature to 900 °C; that is, the temperature coefficient of the conductivity is smaller than that of standard metals. Thus, the results indicate that $LaCo_{0.5}Ni_{0.5}O_3$ is suitable as a conductive material for electrical wiring at high temperatures in air.

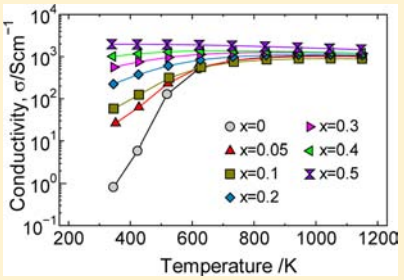

INTRODUCTION

To replace metals in electrical wiring at high temperatures in air, conductive oxides must possess a high electrical conductivity and small temperature dependence, which are comparable to metals. Perovskite-type oxides related to $LaCoO_3$, which have high electrical conductivities and phase stabilities at high temperatures in air,[1] are candidates for such conductive oxides. Sr-doped $LaCoO_3$ is especially promising because it has the highest electrical conductivity among oxides.[2] Although perovskite-type oxides related to $LaCoO_3$ have not received much attention in the field of electronic conductors, they have been investigated in the fields of ionic conductors and magnetism. Because of its high oxide ion diffusivity, $(La,Sr)CoO_3$ doped with Fe to adjust the thermal expansion coefficient has been used as an oxide ion conductor in the cathode of a solid oxide fuel cell (SOFC).[3,4] Moreover, $La_{1-x}Sr_xCoO_3$ exhibits interesting magnetic properties. Increasing the temperature and Sr doping level causes an unusual magnetism. Tokura et al. have suggested an anomalous Hall effect for $0.17 \leq x \leq 0.3$,[5] while Itoh et al. have suggested that $La_{1-x}Sr_xCoO_3$ is a spin glass in the range $0 < x \leq 0.18$ and a cluster glass in the range $x > 0.18$.[6]

Furthermore, improved electrical conductivities and magnetic properties have been realized through Ni doping into Co-sites, and a few earlier reports compared Ni doping to Sr doping into La-sites. From the viewpoint of thermoelectrics, Li et al. have indicated that the electrical conductivity of $LaCo_{1-x}Ni_xO_3$ is elevated to 500 S/cm at 600 K due to an increased carrier concentration by 20 mol % Ni doping, and the power factor of $LaCo_{0.9}Ni_{0.1}O_3$ is about 3.5 times higher than that of undoped $LaCoO_3$.[7] Although it is interesting that $LaCo_{1-x}Ni_xO_3$ has a high electrical conductivity despite the fact that element doping in the Co-sites forms a conduction path, it is difficult to employ $LaCo_{1-x}Ni_xO_3$ in electrical wiring because the temperature coefficient of conductivity is too large. Asai et al. have concluded that Co doping enhances the temperature independent susceptibility of $LaNiO_3$.[8] Glassy ferromagnetism as well as a giant negative magnetoresistance and metal−insulator transition at $x = 0.4$ have been reported for $LaCo_{1-x}Ni_xO_3$.[8,9]

Despite their interesting characteristics, the literature contains fewer reports about $LaCo_{1-x}Ni_xO_3$ compared to $La_{1-x}Sr_xCoO_3$, suggesting further investigations on $LaCo_{1-x}Ni_xO_3$ need to be conducted. To date, the electrical properties for $x > 0.2$ at high temperatures have yet to be examined, and neither the conduction mechanism nor the upper limit of conductivity has yet to be clarified. Thus, it may be possible to further increase the electrical conductivity of $LaCo_{1-x}Ni_xO_3$, which is why we selected $LaCo_{1-x}Ni_xO_3$ as a research target. To clarify the upper limit of the conductivity in $LaCo_{1-x}Ni_xO_3$ and to confirm its applicability for electrical wiring at high temperatures in air, herein the electronic transport properties are investigated through Hall effect measurements, Rietveld analyses, and band-structure calculations.

EXPERIMENTAL SECTION

$LaCo_{1-x}Ni_xO_3$ ($0 \leq x \leq 0.5$) was synthesized by a conventional solid-state technique. Starting powders of $La(OH)_3$ (99.9%, Shin-Etsu Chemical Co., Ltd.), Co_3O_4 (99.9%, Kojundo Chemical Laboratory Co., Ltd.), and NiO (99.9%, Kojundo Chemical Laboratory Co., Ltd.) were weighed in specific proportions and then mixed by ball milling for 15 h using zirconia balls and ethanol. The mixed powders were dried and heated at 1373 K for 2 h in air. The resulting powder was crushed in the ball mill again for 15 h. The powder was dried, pressed into pellets under an isostatic pressure of 147 MPa, and then sintered at 1473−1873 K for 2 h in air.

Received: April 8, 2012
Published: August 16, 2012

   dx.doi.org/10.1021/ic301386s | *Inorg. Chem.* 2012, 51, 9259−9264

The electrical conductivity was measured by the dc four-probe technique using each Pt leg of the thermocouple as the current lead. For Seebeck coefficient measurements in air, a temperature gradient in the specimen was generated by passing air in an alumina protection tube placed near one end of the specimen. The temperature difference between the two ends was controlled to be 2−15 K by varying the flow rate of air. Thermopower measured as a function of the temperature difference produced a straight line and Seebeck coefficient was calculated from its slope. The carrier concentration and mobility were calculated from Hall effect measurements performed at room temperature (Toyo, ResiTest8300), whereas the powder X-ray diffraction (XRD) patterns were measured with Cu Kα radiation at room temperature (Rigaku, RINT TTR-III, $20 \leq 2\theta \leq 120$, step scan 0.02, 50 kV−300 mA). The lattice parameters were refined by Rietveld analyses using the RIETAN2000 code with the powder XRD patterns.

The calculations of the density-of-states (DOS) were conducted based on the hybrid density functional theory by the full-potential APW+lo method using the WIEN2k code.[10−12] The generalized gradient approximation in the scheme of Perdew−Bueke−Ernzerhof (GGA−PBE) with an effective Coulomb parameter (U_{eff}) was used for the exchange-correlation energy.[13] In the APW+lo method, we treated Kr ($4d^{10}$) for La, Ne ($3s^2$) for Co, Ne ($3s^2$) for Ni, and He for O as the electron configuration of the core state. Muffin tin radii were chosen as 2.35, 1.87, 1.87, and 1.66 au for La, Co, Ni, and O, respectively. The summation in the Brillouin zone was performed using 27 000 k-points. The cutoff parameter was set to $R_{mt}K_{max} = 7$. We chose the Coulomb parameter U_{eff} = 5.85 and 6.35 eV for Co and Ni, respectively.[14]

RESULTS AND DISCUSSION

Figure 1a shows the powder XRD patterns of $LaCo_{1-x}Ni_xO_3$. The patterns confirm a single phase of $LaCo_{1-x}Ni_xO_3$ for $0 \leq x \leq 0.2$ was synthesized. Between $0 \leq x \leq 0.2$, $LaCo_{1-x}Ni_xO_3$ forms a complete solid solution and crystallizes as a perovskite-type structure based on a rhombohedral lattice with space group $R\bar{3}c$. Figure 1c shows the crystal structure of $LaCo_{1-x}Ni_xO_3$. However, a small peak of $La_4(Co,Ni)_3O_{10}$ appears near 25.5° as a second phase for $x \geq 0.3$, as shown in Figure 1b.

Rietveld analysis was performed using space group $R\bar{3}c$[15,16] based on a hexagonal lattice. In this analysis, the oxygen content was fixed to 3 (stoichiometric composition), since it is difficult to identify the oxygen content precisely by X-ray diffraction analysis. Table 1 gives the values of the refined parameters for these compositions. The atomic position of O exhibits an anomaly between $0.2 < x < 0.3$, while the hexagonal lattice parameters of a_H and c_H increase as the Ni content increases. To inspect these behaviors upon perovskite block, the parameters converted to the rhombohedral lattice are shown in Figure 2a. Lattice parameter, a, increases as the Ni content increases. In contrast, lattice parameter, α, becomes saturated between $0.3 \leq x \leq 0.5$ but increases between $0 \leq x \leq 0.2$. Both a and α vary monotonically with Ni content, whereas the B−O bond length and the B−O−B bond angle are discontinuous and exhibit anomalies between $0.2 < x < 0.3$ as shown in Figure 2b. The B−O bond length increases with increasing x between $0 \leq x \leq 0.2$, abruptly decreases between $0.2 < x < 0.3$, and increases again between $0.3 \leq x \leq 0.5$. On the other hand, the B−O−B bond angle sharply increases from 164 to 166° as the Ni content increases between $0.2 < x < 0.3$. That is, the BO_6 octahedra connected by sharing vertex oxygen ions are distorted between $0.2 < x < 0.3$ although the lattice parameters increase continuously between $0 \leq x \leq 0.5$. In other words, only the manner of the linkage of BO_6 octahedra is transformed between $0.2 < x < 0.3$ without changing the lattice volume. In addition, the bond-valence-sum (BVS) for B-site

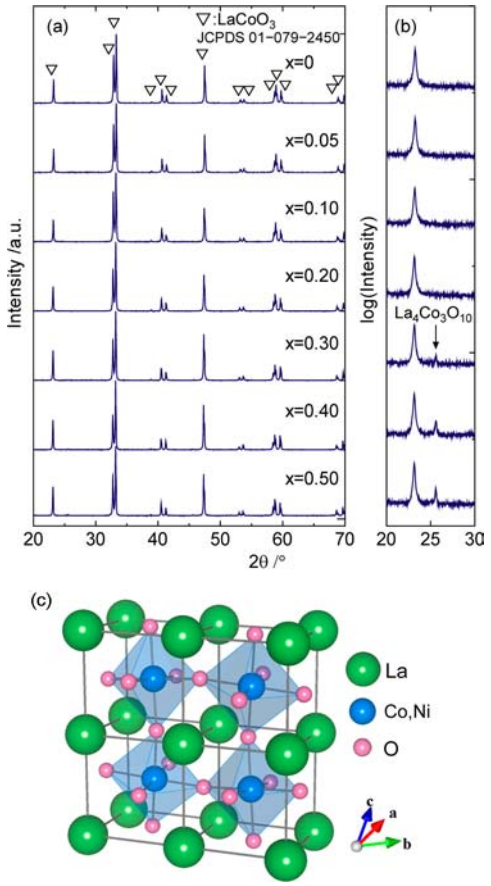

Figure 1. (a) X-ray diffraction patterns of $LaCo_{1-x}Ni_xO_3$ ($0 \leq x \leq 0.5$) and (b) enlarged view by the log scale between $20 \leq \theta \leq 30°$. (c) Crystal structure of $LaCo_{1-x}Ni_xO_3$ based on a rhombohedral lattice.

ions also exhibits the anomaly between $0.2 < x < 0.3$ and sharply increases for $x > 0.3$, as shown in Figure 2c.This is so impressive because the BVS should essentially decrease as Ni^{2+} content increases; that is, Co^{3+} content decreases. On the basis of the anomalies, we surmise that the valence of Ni is 2+ for $x \leq 0.2$ and 3+ for $x \geq 0.3$ judging from the difference in ionic radius (i.e., $Ni^{2+} > Ni^{3+}$), as shown by XANES in an earlier report.[17]

Figure 3 shows the electrical conductivity, σ, at room temperature and the Seebeck coefficient, S, at 343 K as a function of Ni content. σ increases 4 orders of magnitude as the Ni content increases and reaches a maximum of 1.9×10^3 S/cm at $x = 0.5$. Compared to reported values,[7,17] this value is unexpectedly high for $LaCo_{1-x}Ni_xO_3$[7,17] and is the highest value among oxides. In this sense, $LaCo_{1-x}Ni_xO_3$ is very attractive as a highly conductive material. S of $LaCo_{1-x}Ni_xO_3$ shows a maximum value of 230 μV/K at $x = 0.05$ and gradually decreases as the Ni content increases. S approaches zero at $x = 0.5$, and the sign goes from negative to positive between $0 < x < 0.05$ by Ni doping. Our pure $LaCoO_3$ is n-type, though the sign of $LaCoO_3$ remains as a matter to be discussed further.[1,18,19,22]

To analyze the electronic transport properties, the carrier concentration, n, and the carrier mobility, μ, were evaluated by Hall effect measurements at room temperature, as shown in Figure 4. Between $0 < x < 0.05$ where the S changes its sign, the Hall coefficient is reversed from negative to positive, indicating $LaCo_{1-x}Ni_xO_3$ ($0.05 \leq x \leq 0.5$) is a p-type conductor and $LaCoO_3$ is an n-type conductor. Although a flat region is

dx.doi.org/10.1021/ic301386s | Inorg. Chem. 2012, 51, 9259−9264

Table 1. Structural Parameters of $LaCo_{1-x}Ni_xO_3$ Determined by Rietveld Refinement with the Space Group $R\bar{3}c$ Based on a Hexagonal Lattice

parameter		x = 0	x = 0.05	x = 0.10	x = 0.20	x = 0.30	x = 0.40	x = 0.50
lattice parameter	a_H (Å)	5.4443(1)	5.4472(1)	5.4526(1)	5.4587(1)	5.4619(1)	5.4651(1)	5.4652(1)
	c_H (Å)	13.0975(1)	13.0986(1)	13.1076(1)	13.1152(1)	13.1198(1)	13.1267(1)	13.1281(1)
unit cell volume	V/(Å^3)	336.20(1)	336.59(1)	337.49(1)	338.43(1)	338.96(1)	339.53(1)	339.58(1)
Wyckoff position/O 18e	x	0.5475(5)	0.5495(7)	0.5497(6)	0.5496(8)	0.5434(7)	0.5431(8)	0.5443(8)
Rp	(%)	7.77	8.24	7.38	10.76	9.73	10.18	9.64
Rwp	(%)	10.93	11.69	10.12	13.69	13.37	14.27	13.94
Re	(%)	6.52	7.29	7.24	7.53	7.42	7.79	7.83

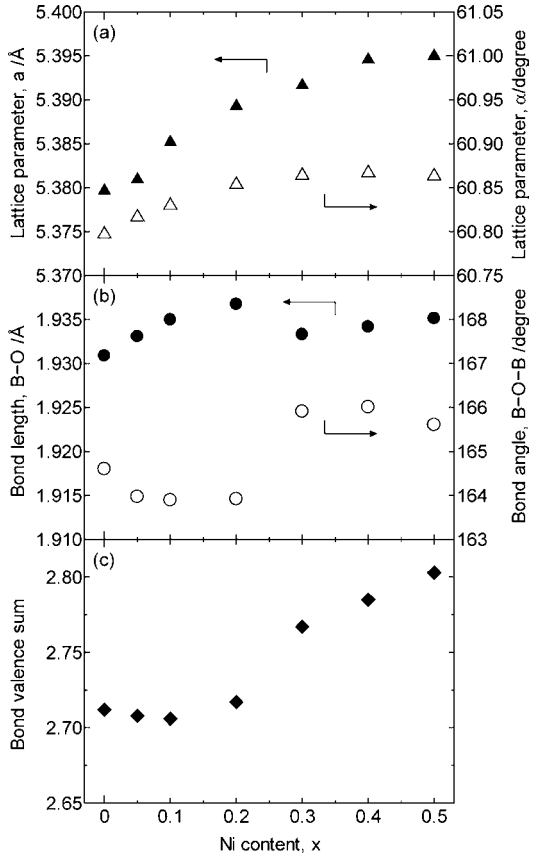

Figure 2. Lattice parameters for $LaCo_{1-x}Ni_xO_3$ based on a rhombohedral unit cell. (a) Lattice constants of a axis and α angle, (b) B−O−B bond angle and B−O bond length, and (c) bond-valence-sum for B-site ions.

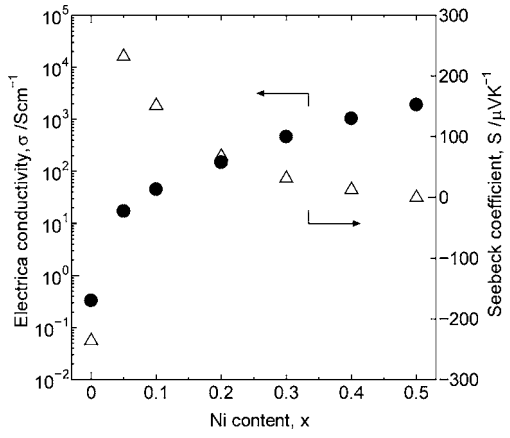

Figure 3. Electrical conductivity, σ, and Seebeck coefficient, S, for $LaCo_{1-x}Ni_xO_3$ at room temperature.

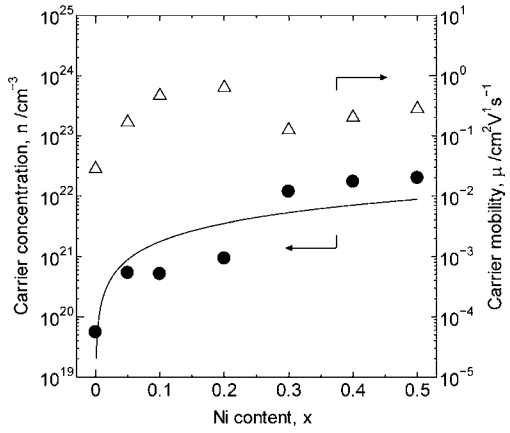

Figure 4. Carrier concentration, n, and carrier mobility, μ, for $LaCo_{1-x}Ni_xO_3$ at room temperature. The solid line indicates the theoretical value of the carrier concentration. (See the text for details.)

observed on the way, n increases as the Ni content increases, reaching a maximum value of 2.2×10^{22} cm^{-3} at x = 0.50, which is extremely high for oxides. For $0 \le x \le 0.2$, the experimental n is less than the theoretical n which is shown in Figure 4 as the solid line. The theoretical n was derived from Ni concentration based on eq 1 and the lattice volume calculated using the lattice parameters as shown in Figure 2a. The oxygen content of $LaCo_{0.8}Ni_{0.2}O_3$ is 2.93, which was estimated on the assumption that the difference between the theoretical and experimental value of the carrier concentration corresponds to carrier generation by oxygen nonstoichiometry based on eqs 1 and 2.

$$Co_{Co}^{\times} + NiO + \frac{1}{2}O_2 \rightarrow Ni_{Co}' + \dot{h} + \frac{1}{2}Co_2O_3 \qquad (1)$$

$$O_O^{\times} \rightarrow \frac{1}{2}O_2 + V_O^{\bullet\bullet} + 2e' \qquad (2)$$

This value is nearly consistent with the value of 2.90 evaluated via iodometric titration, indicating that hole generation caused by Ni doping is in a trade-off relationship with electron generation (i.e., hole "annihilation") by oxygen deficiency for $0 \le x \le 0.2$. An oxygen deficiency appears to be unusual for p-type oxides because p-type oxides should have excess oxygen to generate holes. Moreover, a_H, c_H, and atomic position x of O for $LaCo_{0.8}Ni_{0.2}O_3$, refined by Rietveld analysis taking account of the oxygen content of 2.90 as measured by iodometric titration, are 5.4585 Å, 13.1150 Å, and 0.5494(8), respectively. These values are coincident with those obtained for x = 0.2

dx.doi.org/10.1021/ic301386s | Inorg. Chem. 2012, 51, 9259−9264

with the estimated oxygen content of 3.0 (Table 1 and Figure 2), and we believe the carrier generation would take place according to eqs 1 and 2.

By contrast, the experimental n exceeds the theoretical n for $0.3 \leq x \leq 0.5$. Considering the bond-valence-sum for B-site ions, we surmise that the enhanced carrier concentration for $0.3 \leq x \leq 0.5$ originates in the mean valence of B-site ions.

On the other hand, μ of $LaCo_{1-x}Ni_xO_3$ is less than that of $La_{1-x}Sr_xCoO_3$ for $0.3 \leq x \leq 0.4$.[1] μ increases between $0 \leq x \leq 0.2$ and reaches a maximum value of 0.63 $cm^2/(V\,s)$ at $x = 0.2$. Thereafter, μ decreases between $0.2 < x < 0.3$ but increases between $0.3 \leq x \leq 0.5$. Consequently, the upper limit of the electrical conductivity, σ, of $LaCo_{1-x}Ni_xO_3$ is restricted by the insufficient carrier mobility despite a sufficiently high carrier concentration. Comparing Figures 2b and 4 indicates the carrier behavior, which is the concentration and mobility as a function of Ni content, is similar to that of the BO_6 octahedra, which is the B−O bond length and the B−O−B bond angle. All these parameters show anomalies between $0.2 < x < 0.3$.

In terms of crystal structure, the modulation in BO_6 octahedral chains in the $LaCo_{1-x}Ni_xO_3$ phase and the generation of the $La_4Co_3O_{10}$ phase at grain boundaries can be considered as reasons for the anomalies between $0.2 < x < 0.3$. On the other hand, combing the Hall effect measurement and the bond-valence-sum for B-site ions, it is understood that itinerant carriers are highly concentrated to B-site ions in $LaCo_{1-x}Ni_xO_3$ for $x \geq 0.3$. Hence, we believe that the carriers flow through BO_6 octahedral chains in $LaCo_{1-x}Ni_xO_3$ of a main phase, and this causes the modulation of BO_6 octahedral chains. In addition, the carrier density around Ni is higher than Co as was partly verified by XANES.[17]

To analyze the behavior of the carrier mobility, μ, in more detail, the DOS effective mass, m^*, and relaxation time, τ, were

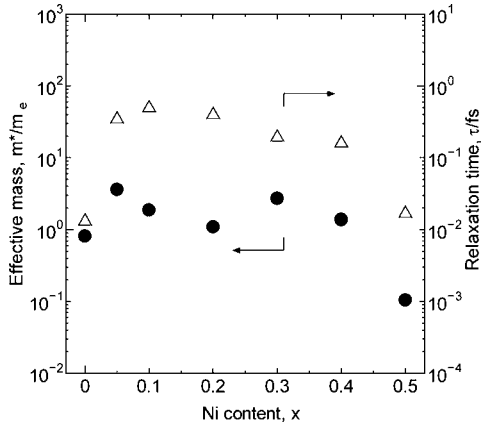

Figure 5. Effective mass, m^*, and relaxation time, τ, for $LaCo_{1-x}Ni_xO_3$ at room temperature.

deduced from S, n, and μ as shown in Figure 5. m^* is estimated using the following equations[20] and the observed S.

$$m^* = \frac{h^2}{2k_BT}\left[\frac{n}{4\pi F_{1/2}(\xi)}\right]^{2/3} \quad (3)$$

$$F_r(\xi) = \int_0^\infty \frac{x^r}{1 + e^{x-r}}\,dx \quad (4)$$

$$S = -\frac{k_B}{e}\left[\frac{(r+2)F_{r+1}(\xi)}{(r+2)F_r(\xi)} - \xi\right] \quad (5)$$

$$\mu = \frac{qT}{m^*} \quad (6)$$

where h, k_B, T, F_r, ξ, r, and q are the Planck constant, Boltzmann constant, absolute temperature, Fermi integral, chemical potential, carrier scattering parameter of the relaxation time, and electric charge, respectively. In this derivation, ionized impurity scattering ($r = 2$) was assumed to be the scattering mechanism by referring to an earlier report concerning $La_{1-x}Sr_xCoO_3$.[1] The m^* value displays an anomaly between $0.2 < x < 0.3$, indicating that the anomaly of the m^* value depends on the increase in the B−O−B bond angle of the BO_6 octahedra. Between $0.3 \leq x \leq 0.5$, m^* decreases as the Ni content increases and m^* reaches 0.10 m_e, where m_e is the free electron mass, at $x = 0.5$, which is sufficiently small. In contrast, τ does not exhibit an anomaly between $0.2 < x < 0.3$. τ decreases as the Ni content increases between $0.1 \leq x \leq 0.5$ and reaches 1.7×10^{-2} fs at $x = 0.5$. It is suggested that the aforementioned small μ is due to the insufficient τ value at $x = 0.5$ where the electrical conductivity reaches a maximum. Here, the carrier scattering parameter has a negligible effect on m^* and μ where the Seebeck coefficient is almost zero, i.e., for $x = 0.5$.

Figure 6a shows the electrical conductivities of the $LaCo_{1-x}Ni_xO_3$ samples measured at 373−1073 K in air. The

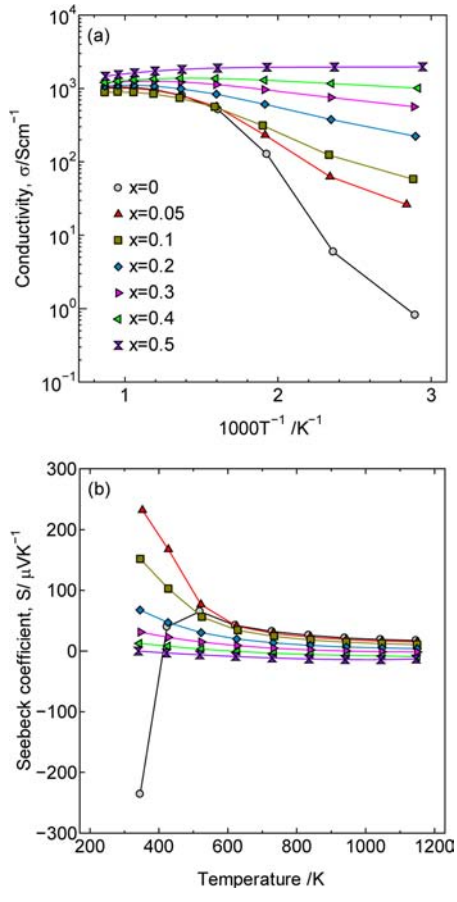

Figure 6. Temperature dependence of (a) electrical conductivity, σ, and (b) Seebeck coefficient, S, for $LaCo_{1-x}Ni_xO_3$.

dx.doi.org/10.1021/ic301386s | Inorg. Chem. 2012, 51, 9259−9264

conductivities for $x \leq 0.4$ exhibit semiconducting behavior below 800 K but become saturated above 800 K. The conductivities for $0.2 \leq x \leq 0.4$ obey an Arrhenius law below 800 K, whereas that for $x \leq 0.1$ do not obey showing an anomaly at 423 K. In contrast, the conductivity for $x = 0.5$ shows the largest value and is metallic over the entire temperature range examined, i.e., the electrical conductivity monotonically decreases as the temperature increases. Furthermore, the temperature coefficient of conductivity for $x = 0.5$ is smaller than that of standard metals, indicating that is suitable for electrical wiring at high temperatures in air.

Meanwhile, the behavior of S of $LaCo_{1-x}Ni_xO_3$ is also interesting. Figure 6b shows the temperature dependence of S, which decreases and reverses its sign from positive to negative as the Ni content and temperature increase. Between $0.4 \leq x \leq 0.5$, $|S|$ remains close to zero even at high temperatures because m^* is close to zero and the temperature coefficient is small, indicating that the electronic structure is maintained from room temperature to 1073 K. On the other hand, the S for $x \leq 0.1$ exhibit an anomaly at 423−523 K. Combining with the behavior of σ for $x \leq 0.1$, which does not obey Arrhenius law owing to an anomaly at 423 K, the change in the electronic structure, i.e., the density-of-states effective mass, is suggested. In addition, the variation of thermogravimetry for $LaCo_{0.5}Ni_{0.5}O_3$ from room temperature to 1173 K is less than 0.05 mass %; that is, little change in oxygen content occurs, in contrast to $La_{1-x}Sr_xCoO_3$.[21] This indicates $LaCo_{0.5}Ni_{0.5}O_3$ is stable even at high temperatures in air. For $x = 0$, the sign of the Seebeck coefficient changes from negative to positive between 340 and 420 K, though the sign of $LaCoO_3$ remains as a matter to be discussed further.[1,18,19,22]

To elucidate the change in the sign of S, the total density-of-states (TDOS) for $LaCo_{0.5}Ni_{0.5}O_3$ was calculated by the hybrid density functional theory utilizing the full-potential APW+lo method using WIEN2k code as indicated in Figure 7a.[15−17] Owing to the contribution to the Fermi level, E_F, of the Ni 3d orbital, the DOS for $LaCo_{0.5}Ni_{0.5}O_3$ is not necessarily consistent with the schematic diagram of electronic structure[22] and the DOS[23,24] for $LaCoO_3$. Contribution of Ni orbital to the DOS is consistent with the spin-state transition upon Ni doping to $LaCoO_3$ described by Hammer et al.[8] We consider this causes the high electronic conduction of $LaCo_{0.5}Ni_{0.5}O_3$; that is, the difference in the electrical properties between $LaCoO_3$ and $LaCo_{0.5}Ni_{0.5}O_3$. The contribution of down-spin to the conduction is small because the E_F lies in the band gap. In the up-spin, TDOS does not possess a band gap at E_F, indicating that $LaCo_{0.5}Ni_{0.5}O_3$ is a half-metal. Ni 3d contributes to the valence band more intensely than Co 3d, suggesting that the itinerant carriers are highly concentrated to Ni; that is, Ni^{3+} ions are formed. In the actual DOS, the shift of E_F to the lower energy side due to high hole concentration content is suggested, although this is a simulation for an ideal stoichiometric composition. Additionally, we calculated the relation between the n and S, from the TDOS in the up-spin using the BoltzTraP code based on the semiclassical Boltzmann theory[25] to clarify the influence of DOS on S. As shown in Figure 7b, S decreases as n increases between $2.0 \times 10^{21} < n < 2.8 \times 10^{22}$ (cm^{-3}), which includes the observed carrier concentration, resulting in S changing from positive to negative at $n = 2.2 \times 10^{22}$ cm^{-3}. Consequently, it is concluded that the change in sign of S originates from the shift of E_F to the lower energy side; that is, the increase in n is caused by Ni doping and elevated temperature.

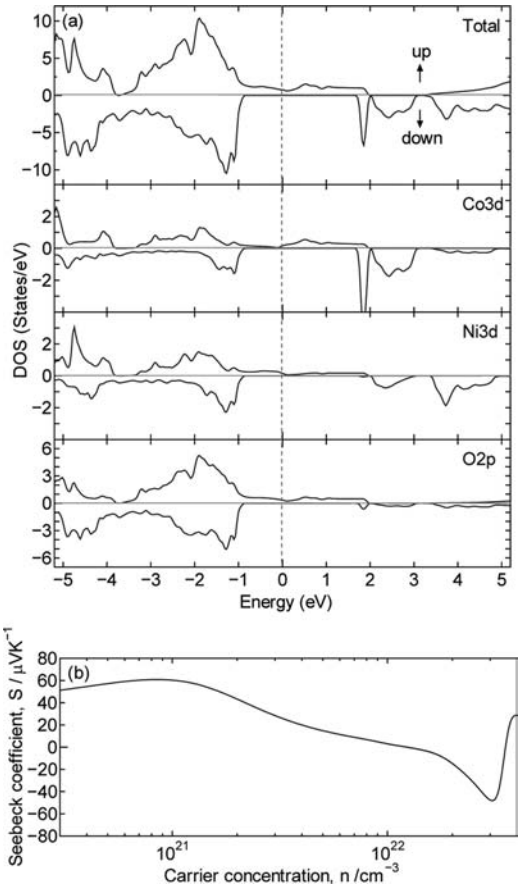

Figure 7. (a) Density-of-states (DOS) for $LaCo_{0.5}Ni_{0.5}O_3$ calculated by the GGA+U method. (b) Relation between the carrier concentration, n, and Seebeck coefficient, S, calculated from the TDOS for the up-spin.

CONCLUSIONS

A high electrical conductivity, σ, of 1.9×10^3 S/cm is achieved for $LaCoO_3$ by 50 mol % Ni doping into Co sites at room temperature. This conductivity is maintained up to 1173 K. The high σ of $LaCo_{0.5}Ni_{0.5}O_3$ can be attributed to the high carrier concentration, n, of 2.2×10^{22} cm^{-3}, and small effective mass, m^*, of 0.1 m_e, but the relaxation time is insufficient for a highly conductive oxide material. The high n originates from the mean valence of B-site ions for $x \geq 0.3$. The carrier mobility, μ, n, m^*, and the mean valence of the B-site ions depend on the B−O−B bond angle and the B−O bond length of the BO_6 octahedra, namely, the manner of modulations of BO_6 octahedral chains. Both the bond angle and the bond length display anomalies in their composition dependencies between $0.2 < x < 0.3$. In contrast, m^* originates from the upper limit of the flat valence band. Furthermore, the temperature coefficient of conductivity of $LaCo_{0.5}Ni_{0.5}O_3$ is smaller than that of standard metals. In conclusion, $LaCo_{0.5}Ni_{0.5}O_3$ is suitable for electrical wiring at high temperatures in air due to its high electrical conductivity, small temperature dependence, and phase stability.

AUTHOR INFORMATION

Corresponding Author

*E-mail: h-kozuka@mg.ngkntk.co.jp. Phone: +81 568 76 1362. Fax: +81 568 76 5274.

Notes

The authors declare no competing financial interest.

dx.doi.org/10.1021/ic301386s | Inorg. Chem. 2012, 51, 9259−9264

■ ACKNOWLEDGMENTS

We are grateful to Dr Y. F. Wang for his advice in Hall effect mesurements and Dr. R. Z. Zhang for his advice in band calculations.

■ REFERENCES

(1) Iwasaki, K.; Ito, T.; Nagasaki, T.; Arita, Y.; Yoshino, M.; Matsui, T. *J. Solid State Chem.* **2008**, *181*, 3145.
(2) Kriener, M.; Zobel, C.; Reichl, A.; Baier, J.; Cwik, M.; Berggold, K.; Kierspel, H.; Zabara, O.; Freimuth, A.; Lorenz, T. *Phys. Rev. B* **2004**, *69*, 094417.
(3) Wang, W. G.; Mogensen, M. *Solid State Ionics* **2005**, *176*, 457.
(4) Tietz, F.; Haanappel, V. A. C.; Mai, A.; Mertens, J.; Stöver, D. *J. Power Sources* **2006**, *156*, 20.
(5) Onose, Y.; Tokura, Y. *Phys. Rev. B* **2006**, *73*, 174421.
(6) Itoh, M.; Natori, I.; Kubota, S.; Motoya, K. *J. Phys. Soc. Jpn.* **1994**, *63*, 1486.
(7) Li, F.; Li, J. F. *Ceram. Int.* **2011**, *37*, 105.
(8) Asai, K.; Sekizawa, H.; Mizushima, K.; Iida, S. *J. Phys. Soc. Jpn.* **1977**, *43*, 1093.
(9) Hammer, D.; Wu, J.; Leighton, C. *Phys. Rev. B* **2004**, *69*, 134407.
(10) Schwarz, K.; Blaha, P.; Madsen, G. K. H. *Comput. Phys. Commun.* **2002**, *147*, 71.
(11) Sjöstedt, E.; Nordström, L.; Singh, D. *J. Solid State Commun.* **2000**, *114*, 15.
(12) Madsen, G. K. H.; Blaha, P.; Schwarz, K.; Sjöstedt, E.; Nordström, L. *Phys. Rev. B* **2001**, *64*, 195134.
(13) Perdew, J. P.; Burke, K.; Ernzerhof, M. *Phys. Rev. Lett.* **1996**, *77*, 3865.
(14) Yang, Z.; Huang, Z.; Ye, L.; Xie, X. *Phys. Rev. B* **1999**, *60*, 15674.
(15) Radaelli, P. G.; Cheong, S. W. *Phys. Rev. B* **2002**, *66*, 094408.
(16) Thornton, G.; Tofield, B. C.; Hewat, A. W. *J. Solid State Chem.* **1986**, *61*, 301.
(17) Wu, T.; Wu, G.; Chen, X. H. *Solid State Commun.* **2008**, *145*, 293.
(18) Berggold, K.; Kriener, M.; Zobel, C.; Reichl, A.; Reuther, M.; Müller, R.; Freimuth, A.; Lorenz, T. *Phys. Rev. B* **2005**, *72*, 155116.
(19) Maignan, A.; Flahaut, D.; Hébert, S. *Eur. Phys. J. B* **2004**, *39*, 145.
(20) Vining, C. B. *J. Appl. Phys.* **1991**, *69*, 331.
(21) Mizusaki, J.; Mima, Y.; Yamauchi, S.; Fuei, K. *J. Solid State Chem.* **1989**, *80*, 102.
(22) Senaris-Rodriguez, M. A.; Goodenough, J. B. *J. Solid State Chem.* **1995**, *116*, 224.
(23) Korotin, M. A.; Ezhov, S. Yu.; Solovyev, I. V.; Anisimov, V. I.; Khomskii, D. I.; Sawatzky, G. A. *Phys. Rev. B* **1996**, *54*, 5309.
(24) Kníže k, K.; Jirák, Z.; Hejtmánek, J.; Novák, P. *J. Phys.: Condens. Matter* **2006**, *18*, 3285.
(25) Madsen, G. K. H.; Singh, D. *J. Comput. Phys. Commun.* **2006**, *175*, 67.